DEVELOPMENT OF SURFACE PLASMONS/ELECTRO OPTIC DEVICES FOR ACTIVE CONTROL OF OPTICAL CHARACTERISTICS

Milan C. Buncick
AEgis Technologies Group, 631 Discovery Dr., Huntsville, AL 35806,
Paul R. Ashley, M. Scalora, and Neset Akozbek
Charles M. Bowden Research Center, AMSRD-AMR-WS-ST, RDECOM, Redstone Arsenal, AL 35898-5000

Maria Antonietta Vincenti
Dipartimento di Energetica, University of Rome La Sapienza, Via Scarpa 16, Rome Italy
Marco Centini
Dipartimento di Energetica, University of Rome La Sapienza, Via Scarpa 16, Rome Italy

Jason D. Fowlkes and Ilia N. Ivanov
Center for Nanophase Materials Sciences
Oak Ridge National Laboratory, PO Box 2008
Oak Ridge TN 37831-6493

ABSTRACT—

We are designing and fabricating arrays of subwavelength SP structures in metal films and combining these structures with EO polymers to understand the interaction of the EO polymer with the enhanced electric fields of the plasmons. We have designed and modeled resonance structures to maximize extraordinary transmittance. We are making a systematic study of SP structure shapes by studying circular holes, elliptical holes and slits. Initially we have fabricated and begun optical evaluation of subwavelength slits in gold films. Slits with 32 nm width and 120nm width have been fabricated by a focused ion beam system. Preliminary optical transmittance measurements in the visible and NIR are underway and will be compared to theoretical modeling.

INTRODUCTION

Surface plasmons (SPs) are of interest to a wide spectrum of scientists, ranging from physicists, chemists and materials scientists to biologists [1]. Renewed interest in SPs comes from recent advances that allow metals to be structured and characterized on the nanometer scale. This in turn has enabled us to control SP properties to reveal new aspects of their underlying science and to tailor them for specific applications.

SP-based photonics are being developed to take advantage of the larger information capacity of an optical communications system over an electronic one while drastically reducing the physical size of components over other optical approaches. In an SP structure, the electromagnetic wave, can propagate along the metal surface in the form of an SP [2]. As a consequence, the fields can be strongly confined to the metal surface with the lateral dimensions much smaller than the wavelength. Therefore, plasmonic circuits possess both the capacity of photonics and miniaturization of electronics, opening a new way for the future applications [3].

SP-based nanophotonics or nanoplasmonics provide a pathway to both control and manipulate optical signals by coupling them to coherent electronic excitations near a metal surface [1]. This has led to the development of a toolbox of various subwavelength photonic components such as mirrors, lenses, plasmonic crystals, and waveguides capable of manipulating plasmonic signals [4]. Moreover, the plasmonic properties of metallic nanostructures determines their conventional optical properties such as reflection, transmission, and absorption. Plasmonic crystals are considered as the basis for superlenses, metamaterials for negative refraction applications, as well as nonlinear metamaterials with enhanced optical nonlinearity [5, 6]. Plasmonic nanostructures are becoming important constituents in light-emitting devices (LEDs, OLEDs, nanolasers), photodetectors, and nanoscale light sources as well as the principle components for future optical data storage, imaging, and sensing. One of the most important yet challenging requirements for applications in photonics, opto-electronics, and optical communications is to introduce a means to control the optical properties of plasmonic devices. To directly influence surface plasmons and hence the associated optical properties, manipulation of the dielectric value of the medium surrounding the plasmonic metal structure can be used to change the resonance condition for light-plasmon coupling. By combining optically nonlinear dielectrics with the metallic structure all-optical control can be accomplished by taking advantage of the intense nature of confined electromagnetic radiation in nanostructured elements [7,8]. Another technique of fundamental importance in the context of controlling the SP resonance is the application of an external electric field [9]. This is especially significant because both plasmonic and electric signals can be guided in the same metallic circuitry. The applied voltage can then be used to exert direct control over an electro optic (EO) dielectric medium changing its refractive index and thus the SP modes at the metal/ dielectric interface.

This research has two purposes: (1) to investigate the affect of the enhanced local field of surface plasmons on EO polymers that surround the plasmonic structures as a function of hole shape and applied voltage and (2) develop plasmonic optical devices using plasmonic structures and EO materials for use in photonic circuits. Using an EO polymer as a host medium we will investigate how nonlinear optical materials and plasmonics structures may be combined to create new devices. In order to take advantage of the EO properties of the polymer, we are designing and building plasmonic devices with resonant

Report Documentation Page

Form Approved
OMB No. 0704-0188

1. REPORT DATE	2. REPORT TYPE	3. DATES COVERED
DEC 2008	**N/A**	**-**

4. TITLE AND SUBTITLE	5a. CONTRACT NUMBER
Development Of Surface Plasmons/Electro Optic Devices For Active Control Of Optical Characteristics	5b. GRANT NUMBER
	5c. PROGRAM ELEMENT NUMBER
6. AUTHOR(S)	5d. PROJECT NUMBER
	5e. TASK NUMBER
	5f. WORK UNIT NUMBER
7. PERFORMING ORGANIZATION NAME(S) AND ADDRESS(ES) **AEgis Technologies Group, 631 Discovery Dr., Huntsville, AL 35806**	8. PERFORMING ORGANIZATION REPORT NUMBER
9. SPONSORING/MONITORING AGENCY NAME(S) AND ADDRESS(ES)	10. SPONSOR/MONITOR'S ACRONYM(S)
	11. SPONSOR/MONITOR'S REPORT NUMBER(S)

12. DISTRIBUTION/AVAILABILITY STATEMENT
Approved for public release, distribution unlimited

13. SUPPLEMENTARY NOTES
See also ADM002187. Proceedings of the Army Science Conference (26th) Held in Orlando, Florida on 1-4 December 2008, The original document contains color images.

14. ABSTRACT

15. SUBJECT TERMS

16. SECURITY CLASSIFICATION OF:			17. LIMITATION OF ABSTRACT	18. NUMBER OF PAGES	19a. NAME OF RESPONSIBLE PERSON
a. REPORT	b. ABSTRACT	c. THIS PAGE			
unclassified	**unclassified**	**unclassified**	**UU**	**4**	

properties in the MWIR and NIR wavebands. We are embedding the plasmonics structures in an EO polymer and measuring their optical response in the mid and near IR waveband. Our intent is to make a systematic study of hole shapes by studying circular holes, elliptical holes with increasing eccentricity and slits. Because the physics of light transmission changes with this variation in shapes we can make a very complete and systematic study of the effects on the EO polymer by the local fields for this plasmonic structure [12-16]. For the first phase of this work we have fabricated slits in gold films.

1. THEORETICAL MODEL

The transmission through a metal substrate having one or more subwavelength apertures is governed by thickness of the metallic substrate, slit size, and inter-slit distance. The structure under consideration consists of gold layer whose dispersion profile is found in Palik's handbook [10], for example. The variation of these parameters is undertaken to enhance the linear transmittance and to begin to appreciate the interaction between the geometrical and physical mechanisms. The calculations and results reported below are obtained by solving Maxwell's equations using three distinct approaches: (1) Commercially available software (FEMALB); (2) A home-grown finite-difference, time-domain (FDTD) algorithm, whose details can be found in reference [11]; and (3) a time-domain fast Fourier transform beam propagation (FFT-BPM) method [12, 13, 14]. Since the FDTD method is the most widely adopted technique, we now outline the FFT-BPM method because it is a potent alternative with significant flexibility [12].

In Gaussian units, the system of equations we aim to solve is as follows:

$$\nabla\times\mathbf{E}=-\frac{1}{c}\frac{\partial\mathbf{B}}{\partial t} \qquad \nabla\times\mathbf{H}=\frac{1}{c}\frac{\partial\mathbf{E}}{\partial t}+\frac{4\pi}{c}\frac{\partial\mathbf{P}}{\partial t}$$
$$\ddot{\mathbf{P}}+\gamma\dot{\mathbf{P}}=\frac{\omega_p^2}{4\pi}\mathbf{E} \qquad (1)$$

We assume a right-handed coordinate system, and $\hat{p}$-polarized (TM) pump field of the form:

$$\mathbf{E}=\mathbf{j}\left(E_y^{\omega}e^{-i\omega t}+\left(E_y^{\omega}\right)^{*}e^{i\omega t}\right)+\mathbf{k}\left(E_z^{\omega}e^{-i\omega t}+\left(E_z^{\omega}\right)^{*}e^{i\omega t}\right) \qquad (2)$$
$$\mathbf{H}=\mathbf{i}\left(H_x^{\omega}e^{-i\omega t}+\left(H_x^{\omega}\right)^{*}e^{i\omega t}\right)$$

The corresponding macroscopic polarization is given by:

$$\mathbf{P}=P_y\mathbf{j}+P_z\mathbf{k}=\mathbf{j}\left(P_y^{\omega}e^{-i\omega t}+\left(P_y^{\omega}\right)^{*}e^{i\omega t}\right)+\mathbf{k}\left(P_z^{\omega}e^{-i\omega t}+\left(P_z^{\omega}\right)^{*}e^{i\omega t}\right) \quad (3).$$

The envelope functions E_y^{ω}, E_z^{ω}, H_x^{ω}, P_y^{ω}, P_z^{ω} contain implicit spatial dependences that for simplicity have been omitted. In addition, the envelope functions are not assumed to be slowly varying, as no approximations are made when the fields and polarizations are substituted into Maxwell's equations. In other words, the decomposition of the fields in Eqs.(2-3) is a matter of mere convenience. Substitution of Eqs.(2-3) into Eqs.(1) results in a system of seven coupled differential equations for the fields, polarizations, and corresponding currents, which in scaled form are written as follows:

$$\frac{\partial H_x^{\omega}}{\partial\tau}=i\beta\left(H_x^{\omega}+E_z^{\omega}\sin\theta_i+E_y^{\omega}\cos\theta_i\right)-\frac{\partial E_z^{\omega}}{\partial\tilde{y}}+\frac{\partial E_y^{\omega}}{\partial\xi}$$
$$\frac{\partial E_y^{\omega}}{\partial\tau}=i\beta\left(E_y^{\omega}+H_x^{\omega}\cos\theta_i\right)+\frac{\partial H_x^{\omega}}{\partial\xi}-4\pi(J_y^{\omega}-i\beta P_y^{\omega})$$
$$\frac{\partial E_z^{\omega}}{\partial\tau}=i\beta\left(E_z^{\omega}+H_x^{\omega}\sin\theta_i\right)-\frac{\partial H_x^{\omega}}{\partial\tilde{y}}-4\pi(J_z^{\omega}-i\beta P_z^{\omega})$$
$$\frac{\partial J_y^{\omega}}{\partial\tau}=\left(2i\beta-\gamma_{\omega}\right)J_y^{\omega}+\left(\beta^2+i\gamma_{\omega}\beta\right)P_y^{\omega}+\frac{\pi\omega_{p,\omega}^2}{\omega_r^2}E_y^{\omega} \qquad (4)$$
$$\frac{\partial J_z^{\omega}}{\partial\tau}=\left(2i\beta-\gamma_{\omega}\right)J_z^{\omega}+\left(\beta^2+i\gamma_{\omega}\beta\right)P_z^{\omega}+\frac{\pi\omega_{p,\omega}^2}{\omega_r^2}E_z^{\omega}$$
$$J_y^{\omega}=\frac{\partial P_y^{\omega}}{\partial\tau} \qquad J_z^{\omega}=\frac{\partial P_z^{\omega}}{\partial\tau}$$

We have chosen λ_r =1μm as the reference wavelength, and have adopted the following scaling: $\xi=z/\lambda_r$ and $\tilde{y}=y/\lambda_r$ are the scaled longitudinal and transverse coordinates, respectively; $\tau=ct/\lambda_r$ is the time in units of the optical cycle; $\beta=2\pi\tilde{\omega}$ is the scaled wave vector; $\tilde{\omega}=\omega/\omega_r$ is the scaled frequency, and $\omega_r=2\pi c/\lambda_r$, where c is the speed of light in vacuum. θ_i is the angle of incidence of the pump with respect to the normal direction. The linear dielectric response of silver has been assumed to be Drude-like, as follows: $\varepsilon(\tilde{\omega})=1-\frac{\omega_P^2}{\tilde{\omega}^2+i\gamma\tilde{\omega}}$. This function is then fitted to the data at any given wavelength. For example, at 800nm, the actual data [Palik] is fitted using the set of parameters: $(\gamma_{\omega},\omega_{p,\omega})$=(0.06, 6.73). The incident magnetic field was assumed to be Gaussian of the form: $\mathcal{H}_x(\tilde{y},\xi,\tau=0)=H_0\,e^{-[(\xi-\xi_0)^2+\tilde{y}^2]/w^2}$, with similar expressions for the transverse and longitudinal electric fields. The equations are then solved in the time domain using the well-known, widely-used split-step algorithm. In short, the propagation is done in two separate steps: first the material interaction is taken into account, and then the fields are propagated in free space. The equations are integrated using a mix of a predictor-corrector algorithm for the material part, and fast Fourier transform for the free space propagation part. The main advantages that the FFT

approach offers over the FDTD method may be summarized as follows: (1) calculation of the spatial derivative is much more accurate; (2) convergence is somewhat more rapid, in part due to the accurate rendition of the spatial derivatives, thus allowing for larger temporal and spatial integration steps; (3) the method is unconditionally stable, and allows one to choose a temporal integration step based on numerical convergence rather than longitudinal or transverse discretization steps.

A plot of the calculated optical transmittance as a function of wavelength is shown in Figure 1. The blue plot is for gold slits with air in the trench. The read plot is for slits filled with a material with index 1.67.

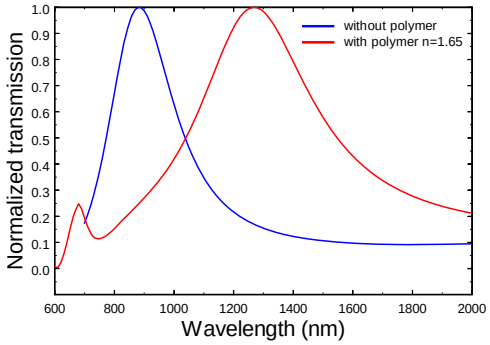

Figure 1. Transmittance versus wavelength for 120 nm slit slits in a gold substrate.

2. SAMPLE PREPARATION

Samples were fabricated by depositing gold films supported on DSP Si wafer, pyrex wafer and glass slides using a Thermionics e-beam evaporation system. Thicknesses were monitored by an Inficon quartz crystal thickness monitor. Gold thicknesses were either 200 nm or 250 nm depending on the particular sample type being fabricated. For this study we made two sets of slits: (1) 33 nm wide slits at a 400 nm pitch in 200 nm gold films and (2) 120 nm slits at a 720 nm pitch in 250 nm gold films. The slits were written by an FEI Nova™ 600 NanoLab DualBeam™ (FIB/SEM) focused ion beam system using a Ga ion beam. For pattern generation the FIB system is controlled by a Raith ELPHY Quantum software/hardware system. The accelerating voltage was 30 keV and the ion current was 30 pA. Single pass milling was used in conjunction with a dwell time of 757 µs for the 32 nm slits and 757 ms for the 120 nm slits. A 16 nm pixel size was used in both cases. The slits were 90 µm long and enough slits were written in each case to give a written area of 90 µm x 90 µm. The pattern for 32 nm wide slits is shown in Figure 2. The 120 nm wide slits are shown in Figure 3.

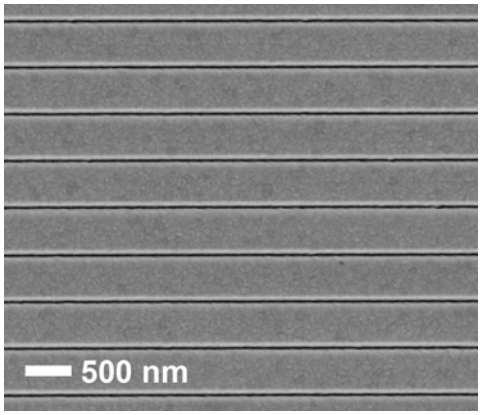

Figure 2. 32nm line arrays (400 nm pitch) patterned in an Au film (~200 nm thick) on DSP Si wafer. The array size is 90 µm x 90 µm.

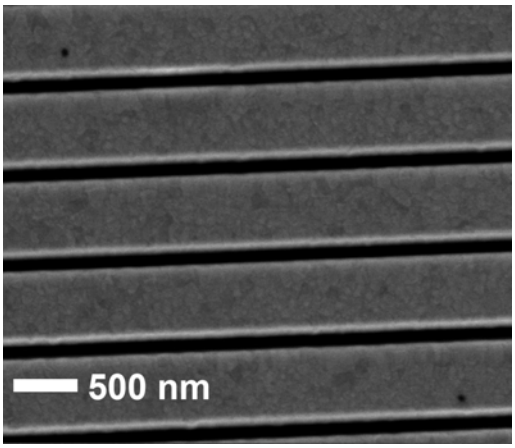

Figure 3. 120nm line arrays (700 nm pitch) patterned in an Au film (~250 nm thick) on DSP wafer. The array size is 90 µm x 90 µm.

After the samples were fabricated and the optical transmittance was measured they were coated with an EO polymer. The polymer is a nitrophenylhydrazone based phenoxy thermoplastic polymer. The material precursor is mixed in a cyclopentanone solvent. For this application is solids concentration was 21%. The solution is spin coated to provide a thin film. It was filtered through a 0.2 micron filter just prior to spin coating. The samples were spun at 1300 RPM for 20 sec on a standard photoresist spin coater. The sample was then baked at 100°C for 10 minutes and then ramped to 140°C over 8 minutes and held at 140°C for 25 minutes. It was then cooled to 30°C and stored in N_2 for 24 hrs before additional optical measurements were made.

3. OPTICAL MEASUREMENTS

Optical measurements were performed using two Ocean Optics spectrometers and a quartz-halogen light source. Because we are interested in the optical response in both the NIR and the mid-IR we used both UV-vis and a NIR spectrometer to cover the waveband from 400-800 nm and 1000-2000 nm. The light source and the spectrometers use

fiber optics with collimating lenses to deliver the light to the sample and collect it from the sample. **Figure 4** shows the optical transmittance as a function of wavelength for 120 nm wide slits in a 250 nm layer of Au. The plot is a combination of the results from the UV-vis spectrometer and the NIR spectrometer.

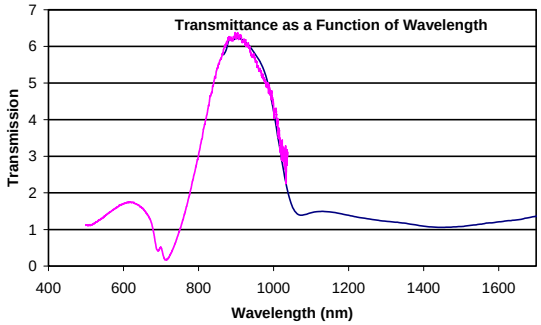

Figure 4: Optical transmittance as a function of wavelength for 120nm slits in 250nm of Au

Figure 5 shows the same sample after the EO polymer has been applied. The peak has been red shifted as predicted by the theory.

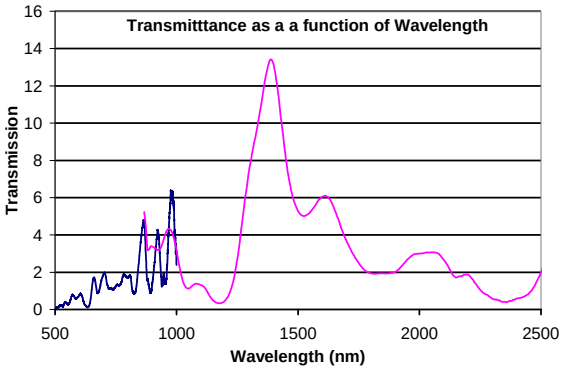

Figure 5: Optical transmittance as a function of wavelength for 120nm slits in 250nm of Au

ACKNOWLEDGMENT

A portion of this research at Oak Ridge National Laboratory's Center for Nanophase Materials Sciences was sponsored by the Scientific User Facilities Division, Office of Basic Energy Sciences, U.S. Department of Energy.

REFERENCES

[1] W.L. Barnes, A. Dereux, and T.W. Ebbesen, “Surface plasmon subwavelength optics,” Nature, vol. 424, pp 824-830, 14 August 2003.

[2] Raether, H. Surface Plasmons (ed. Hohler, G.) (Springer, Berlin, 1988).

[3] Ekmel Ozbay, “Plasmonics: Merging Photonics andElectronics at Nanoscale Dimensions,” *Science vol* 311, pp 189-193 (2006).

[4] A.. Zayats, I.I. Smolyaninov, and A.A. Maradudin, “Nano-optics of surface plasmon polaritons,” Phys. Rep. vol *408, pp* 131-314, 2005.

[5] S.A. Maier, “Plasmonics – Towards Subwavelength Optical Devices,” Current Nanoscience, vol 1pp. 17-22, 2005.

[6] T. W. Ebbesen, H. J. Lezec, H. F. Ghaemi, T. Thio, and P. A. Wolff, “Extraordinary optical transmission through subwavelength hole arrays,” Nature (London) vol. 391, pp 667–669 1998.

[7] G. A. Wurtz, R. Pollard, and A.V. Zayats, “Optical Bistability in Nonlinear Surface-Plasmon Polaritonic Crystals,” PRL vol 97, 057402 2006.

[8] D. Pacifici, H.J. Lezec, and H.A. Atwater, “All-optical modulation by plasmonic excitation of CdSe quantum dots,” Nature photonics vol 1 pp 402-406, July 2007.

[9] T. Nikolajsen, K. Leosson, and S.I. Bozhevolnyi, “Surface plasmon polariton based modulators and switches operating at telecom wavelengths,” App. Phys. Lett., vol 85(24) pp 5833-5835, 2004.

[10] E.D. Palik, "Handbook of Optical Constants of Solids", Academic Press, London-New York (1985).

[11] R.W. Ziolkowski, "Pulsed and CW Gaussian beam interactions withdouble negative metamaterials slab", Opt. Express 11, 662 (2003).

[12] M.C. Larciprete, A. Belardini, M.G. Cappeddu, D. de Ceglia, M. Centini, E. Fazio, C. Sibilia, M.J. Bloemer, M. Scalora, "Second harmonic generation from metallo-dielectric multilayer photonic band gap structures", Phys. Rev. A 77, 013809 (2007)

[13] M. Scalora, G. D'Aguanno, N. Mattiucci, M. J. Bloemer, D. de Ceglia, M. Centini, A. Mandatori, C. Sibilia, N. Akozbek, M. G. Cappeddu, M. Fowler, and J. W. Haus, "Negative refraction and sub-wavelength focusing in the visible range using transparent metallo-dielectric stacks", Opt. Express 15, 508 2007.

[14] M. Scalora, G. D'Aguanno, N. Mattiucci, M.J. Bloemer, J.W. Haus, A.M. Zheltikov, "Negative refraction of ultrashort electromagnetic pulses", Appl. Phys. B 81, 393 2005.